University of Glasgow | Experimental Particle Physics

GLAS-PPE/2009-28
8th December 2009

Department of Physics and Astronomy
Experimental Particle Physics Group
Kelvin Building, University of Glasgow,
Glasgow, G12 8QQ, Scotland
Telephone: +44 (0)141 330 2000 Fax: +44 (0)141 330 5881

LHCb Collaboration LHCb 2009-005

Acceptance effects and background studies in the $B_d \to K^* \mu^+ \mu^-$ decay at LHCb

F Marinho[a,b,*], C Parkes[a], S Viret[a,c]

[*] *Corresponding author*

[a] The University of Glasgow, Dept. of Physics and Astronomy, Glasgow, G12 8QQ.

[b] Now at IFT/UNESP, São Paulo/Brazil

[c] Now at CNRS, Clermont-Ferrand

Abstract

Potential biases on the dimuon mass squared distribution and forward-backward asymmetry (FBA) in the $B_d \to K^* \mu^+ \mu^-$ channel are discussed. Biases due to the offline or trigger selection of the events and due to the mismeasurement of the background distributions were studied. The major contribution to the event selection biases was found to be from the selection applied to muon candidates. A method to study this bias with data is suggested. The sensitivity obtained for the FBA zero crossing point was $\sigma_{S_0} = 0.44\ \mathrm{GeV}^2/\mathrm{c}^4$ for $2\,\mathrm{fb}^{-1}$ data when the background contribution was taken into account. Mismeasurement of the background level can lead to a bias in the FBA, and the asymmetric forward-backward background component should be estimated with an accuracy better than 50 % to prevent biases comparable to the $2\,\mathrm{fb}^{-1}$ statistical sensitivity. These studies were performed using an unbinned FBA analysis.

1 Introduction

This note considers two potential sources of bias on the dimuon mass squared distribution and forward-backward asymmetry (FBA) in the $B_d \to K^*\mu^+\mu^-$ channel. One source of bias comes from the selection of events (offline or in the trigger) for the analysis, this is referred to as the acceptance effect. The other source of bias considered is from the imperfect knowledge of the background level and composition.

A non-parametric unbinned method was developed in [1] to evaluate the FBA distribution of the $B_d \to K^*\mu^+\mu^-$ decay at LHCb. The unbinned method provides access to the dimuon mass squared distributions and to the FBA distribution as continuous curves. A simplified simulation was used to evaluate the LHCb sensitivity to measure the FBA distribution. For an integrated luminosity of 2 fb^{-1}, the FBA zero point sensitivity was determined to be $\sigma_{S_0} = 0.4\,\mathrm{GeV}^2/c^4$. These previous results neglect any contribution from reconstruction, selection and background effects.

In the following sections these effects are discussed. Section 2 discusses the effects of the reconstruction of the particles and event selection on the FBA distribution. Section 3 evaluates the possible effects due to the presence of residual background events in the selected sample. Conclusions are presented in Section 4.

2 Acceptance Effects

This section considers the effect of offline event selection cuts (Section 2.1), muon identification (Section 2.2), and muon momentum cuts in the first level (L0) trigger (Section 2.3) on the reconstructed dimuon mass squared and FBA distributions. The effect is evaluated by considering the acceptance functions: the ratio between the distributions obtained with the selected events from the full LHCb simulation and the generated distributions. An analysis to evaluate acceptance effects directly from data is discussed in Section 2.4.

Simulated events corresponding to ~ 8 fb^{-1} of signal event data were used in this study. These events were generated using the complete LHCb detector simulation. Results of other studies of acceptance effects can be found in [2, 3], these studies focused on the acceptance effects on the θ_l angle[1)].

2.1 Selection Cuts

Events obtained with the LHCb simulation were used to evaluate if any of the selection cuts could potentially bias the dimuon mass distribution and the FBA distribution. The distributions obtained with and without a given cut applied were compared, while the other cuts used in the selection were not altered.

The LHCb event selection described in [4] was used in this study. Figure 1 shows the FBA evaluated with the full LHCb simulation and the distribution obtained with the event generator alone. The black solid line is the FBA obtained after applying all selection cuts and the blue dashed line is the generator level curve. While the lines are in reasonable agreement, there are some regions where the difference between the curves is up to $1.8 - 2\sigma$ for this 8 fb^{-1} sample. The zero point was shifted from the expected position by about $\sim 2\sigma$. While the statistics available were not conclusive as to whether there were significant biases or not, this was the only available sample and was used as a reference to look at the differences introduced by individual cuts.

The comparison between distributions was performed, checking the effect of each cut applied individually to the particles produced in the $B_d \to K^*\mu^+\mu^-$ decay. The selection variables checked are listed below:

[1)] θ_l is the angle between the Bd meson and the positive muon in the dimuon reference frame.

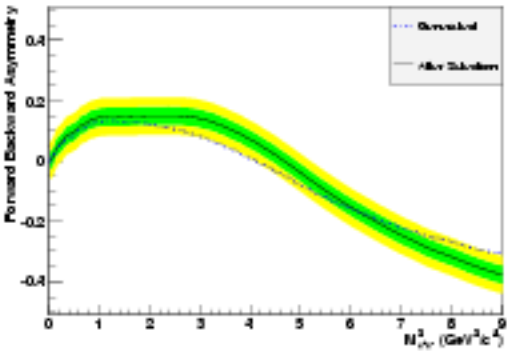

Figure 1: FBA distribution after selection cuts. The blue line is the generator level distribution and the black line is the result obtained with the complete LHCb simulation. The green and yellow areas indicate the 1σ and 2σ regions with an $8\ \text{fb}^{-1}$ simulation sample. The error bands were calculated according to the procedure described in [1].

- P_T: transverse momentum;
- P: absolute momentum;
- IP/σ: impact parameter significance with respect to the primary vertex (PV);
- vertex χ^2: for B_d, K^*, dimuon ;
- $Z_{B_d} - Z_{PV}$: flight distance with respect to the primary vertex (z direction).

From these comparisons only the P_T cuts applied to the single muons were observed to affect the dimuon mass squared distribution. Figure 2 shows the ratio between the normalised dimuon mass squared distributions[2] before and after the muons P_T cut of 500 MeV. A slope as a function of the dimuon mass squared is observed. The difference between the maximum and minimum values of the graphs are $\sim 15 - 18\%$.

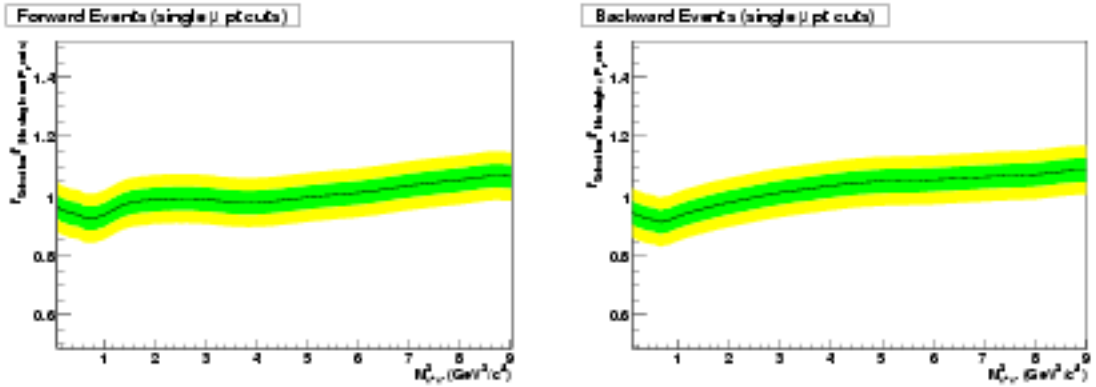

Figure 2: Ratio between the normalised dimuon mass squared distribution before and after the muon P_T cut at selection level. The acceptance effect for the forward events is shown on the left-hand side and for the backward events it is shown on the right-hand side.

The dimuon mass squared distributions obtained with all the selection cuts applied were then scaled with the result shown in figure 2 to apply an acceptance correction. The difference between the

[2] The dimuon mass squared distributions obtained with the unbinned method are normalised. Since $f(M^2) = 1/N \times \sum_{i=1}^{N} K(M^2)$, where K are normalised gaussians, $\int_0^{M^2_{max}} f(M^2)dM^2 = 1/N \times N = 1$ (see [1]).

FBA obtained and the expected curve reduced to $\sim 1.2 - 1.8\sigma$ and the zero point shift was reduced to $\sim 1\sigma$. This suggests that not only is there an effect in the individual distributions as shown in Figure 2 but that this effect differs between the forward events and backward events.

Figure 3 shows the ratios obtained by performing the same procedure but using the cut on P or the cut on IP/σ for the single muons. In both of these cases the distributions obtained were flat and hence no significant effect on the FBA was observed. Similar results were obtained with cuts applied to the dimuons, kaons and pions.

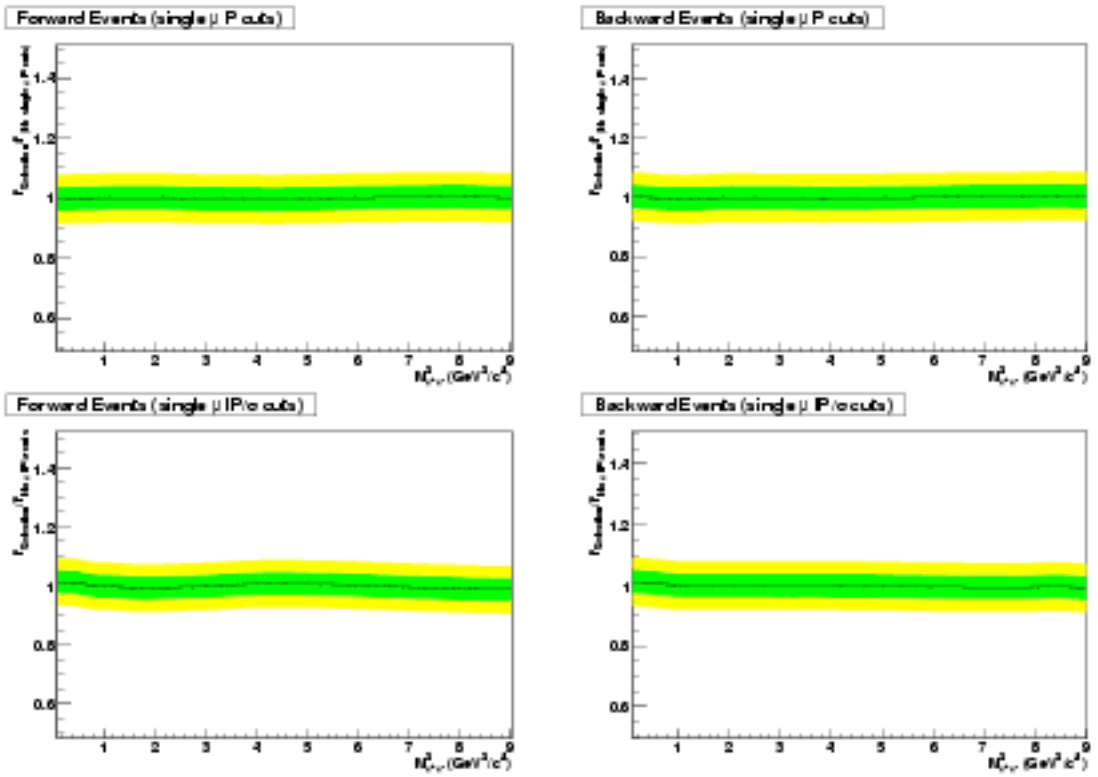

Figure 3: Ratio between the normalised dimuon mass squared distribution before and after the muon P or IP/σ cut at selection level. The acceptance effect for the forward events is shown on the left-hand side and for the backward events it is shown on the right-hand side. No significant acceptance effect was observed.

2.2 Muon Identification

A study of possible acceptance effects due to the muon identification was carried out as a consequence of the effect observed on single muon P_T cuts at selection level (see Section 2.1). This section shows the result obtained by including the muon identification in the analysis.

A variable used to identify muons in the selection is the difference in log-likelihood for muon and pion hypotheses ($DLL(\mu - \pi)$). This variable is calculated by the particle identification algorithms [5]. Figure 4 shows the distribution of the DLL versus P_T and the cuts applied. From this figure it is clear that the DLL and P_T variables are correlated.

By removing the DLL and P_T cuts it was possible to identify their contribution to the acceptance function, keeping the correlation between these two variables. The simulation of the L0 hardware trigger was not included here but is discussed in Section 2.3. Figure 5 shows the ratio between the dimuon mass squared distributions with and without the DLL and P_T cuts. The effect was quantitatively similar to that observed for muon P_T in figure 2 but the deviations were now more pronounced. The difference between the maximum and minimum values of the graphs are $\sim 25 - 30\%$.

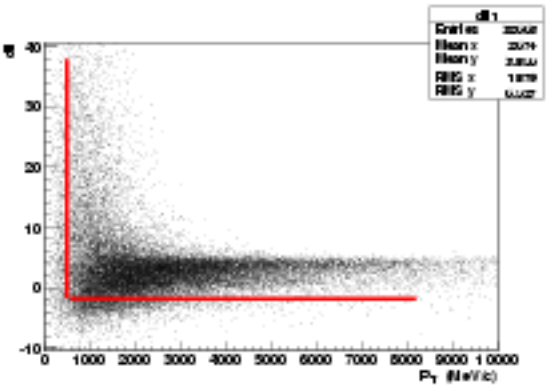

Figure 4: Correlation between muon P_T and DLL variables. Cut values are indicated in the figure ($P_T > 500$ MeV/c and $DLL > -2$).

Again, an acceptance correction can be made by scaling the forward and backward dimuon mass squared distributions by the results shown in figure 5. After applying the correction similar results were obtained when comparing to the case where only the P_T cut was applied. The difference between the obtained and expected FBA curves were smaller than 1.5σ and the zero point shift reduced to $\sim 1\sigma$.

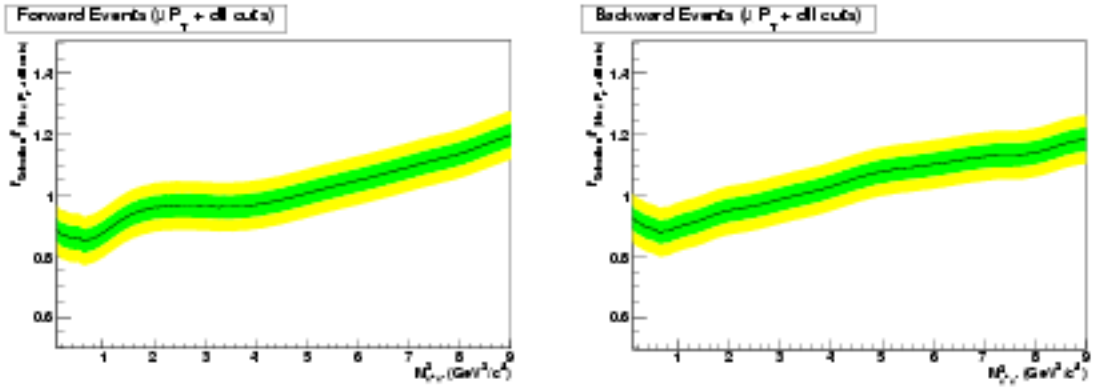

Figure 5: Ratio between the dimuon mass squared distribution before and after the muon P_T and DLL cuts. The acceptance effect for the forward events is shown on the left-hand side and for the backward events it is shown on the right-hand side.

2.3 L0 Trigger

The simplified simulation described in [1] was used to make a rough estimate of the possible effects of the L0 trigger P_T cuts on the acceptance. Two P_T cuts are implemented in the L0 trigger. The event can be accepted if at least one muon candidate has $P_T > 1.2$ GeV/c or if two muon candidates satisfied the constraint $P_T^{\mu_1} + P_T^{\mu_2} > 1.0$ GeV/c [5]. Figure 6 shows the acceptance effect in both cases. The effect of the single muon P_T cut was similar to that observed in the offline event selection reported above. The difference between the maximum and minimum values of the graphs are $\sim 19 - 22\%$. No significant biasing effect was observed from the combined muon P_T cut.

2.4 Proposal for Single Muon Calibration

The acceptance results shown in Sections 2.1, 2.2 and 2.3 suggest that the major component of the acceptance effects in the measured FBA of the $B_d \to K^*\mu^+\mu^-$ decay were due to the cuts applied

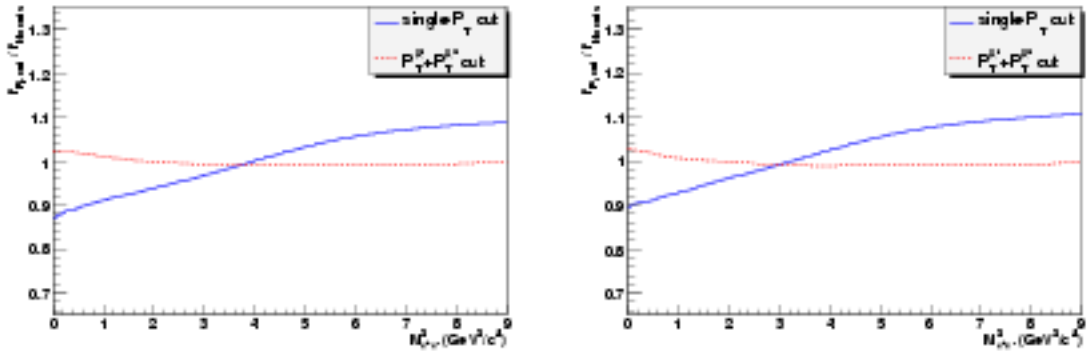

Figure 6: Ratio between the dimuon mass squared distribution before and after the muon P_T cuts on the L0 trigger. The blue solid (red dashed) line shows the acceptance effect due to the single (double) muon P_T cut. The acceptance effect for the forward events is shown on the left-hand side and for the backward events it is shown on the right-hand side.

to single muons. Hence, these effects can be evaluated on a sample of single isolated muons selected from LHCb data. This muon sample should be selected without applying muon identification or momentum cuts. This data set would allow the evaluation of the acceptance effects on single muons and also provide information for the calibration of the LHCb simulation. This section suggests a strategy to select muons for this calibration based on the use of $J/\psi \to \mu^+\mu^-$ samples.

Events selected by the L0 single muon trigger can be used. The particle triggered in L0 can be confirmed as a muon by the muon identification algorithm. Other selection cuts could also be applied to this muon. Then, another particle track with opposite charge can be combined with the identified muon. No particle identification, or biasing selection cuts, should be applied to this charged track. If this combination of particles have a very good vertex fit and the resulting invariant mass is close to the J/ψ mass, then this charged particle is kept as part of the selected muon sample. This sample of muons can then be used for the acceptance effect study.

A simplified version of this method was attempted in order to evaluate its applicability to the $B_d \to K^*\mu^+\mu^-$ decay. The P_T distributions of the muons were obtained with tight and loose muon identification [5]. The resulting distributions were then compared using muons from a $J/\psi \to \mu^+\mu^-$ sample and muons from a signal $B_d \to K^*\mu^+\mu^-$ samples. Figure 7 shows the effect of the DLL cut on the P_T distribution of the muons for these samples. In both samples, the DLL cut introduced an observable effect in the distribution below $4\ \mathrm{GeV/c}$, albeit that the muon spectrum from the J/ψ sample is softer.

In LHCb $\sim 10^9$ $J/\psi \to \mu^+\mu^-$ events will be produced per $2\ \mathrm{fb}^{-1}$ and the statistics available for this study will be very high. However, in order to reduce the contamination of the sample by pions produced in the PV, events of the type $B \to J/\psi(\mu^+\mu^-)X$ can be used. A requirement on the J/ψ vertex being separated from the PV can then be imposed. The statistics available are still large: the total number of events of the type $B \to J/\psi(\mu^+\mu^-)X$ available for the analysis would be of the order of 10^8.

This proposal offers a mechanism for understanding acceptance effects on data. However, further investigation is necessary in order to evaluate the feasibility of this calibration method. Suitable efficiency and background suppression must be demonstrated in the muon selection from $B \to J/\psi(\mu^+\mu^-)X$. It is also necessary to understand how to propagate the acceptance effects on the single muons to the dimuon mass distribution. A method to correctly weight the distributions on an event-by-event basis according to the P_T values of the muons would be required.

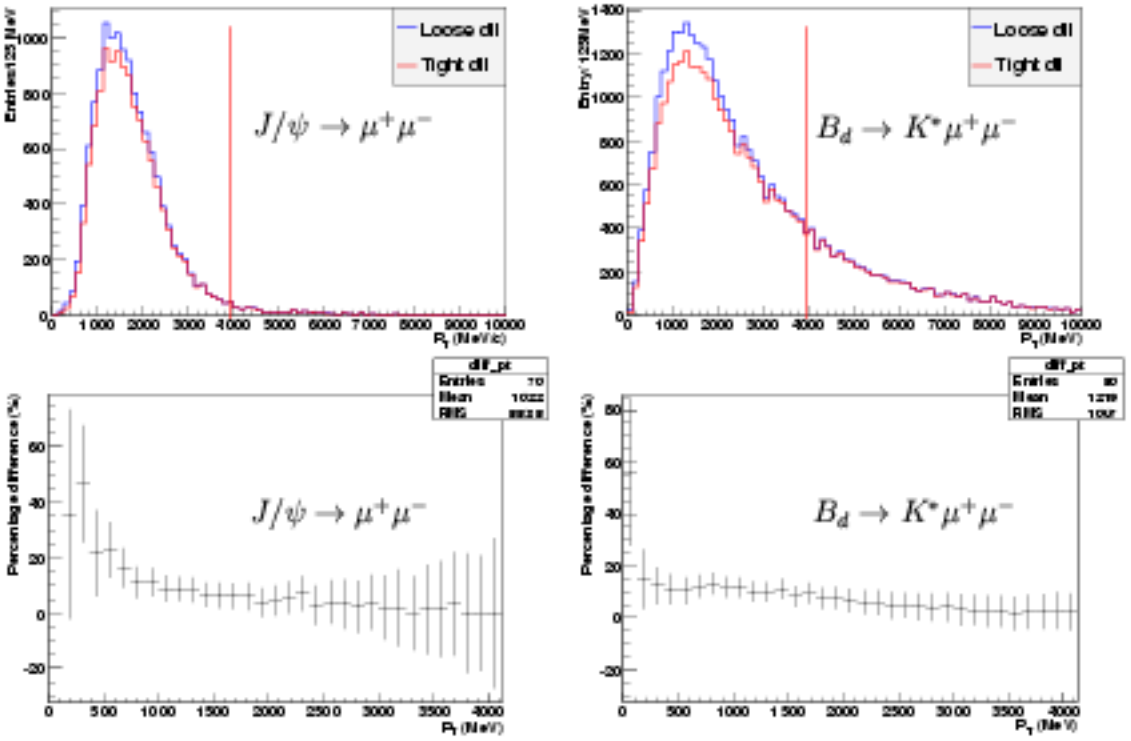

Figure 7: Comparison of muon P_T distributions before and after particle identification. On the top row the P_T distributions loose (blue) and tight (red) the DLL cuts are seen. The bottom row shows the percentage difference between the distributions. The left column shows the graphs obtained with the $J/\psi \to \mu^+\mu^-$ sample and the right column shows the graphs for $B_d \to K^*\mu^+\mu^-$.

3 Background Effects

This section reports the effect of including background events in the FBA distribution measurement. Unfortunately, the background level and contributing channel breakdown is not currently well known from the LHCb simulation. The number of simulated background events available is low when compared to the number of events expected to be produced in LHCb. Given this uncertainty, and the inherent uncertainty at this stage in the reliability of the simulation, this study evaluates the influence on the analysis as the background is varied. The unbinned method described in [1] was adapted in order to perform the background subtraction, as discussed in Section 3.1.

Background simulation studies are reported in [4][3], the total number of background events within the range $0 < \mathrm{M}^2_{\mu^+\mu^-} < 9\ \mathrm{GeV}^2/c^4$ was found to be a factor $\sim 0.30 \pm 0.09$ smaller than the number of signal events in the same $\mathrm{M}^2_{\mu^+\mu^-}$ range (~ 1100 events). The background events were classified according to their θ_l angle distribution. Events where the dimuon was a combination of muons coming from different decays were found to contribute equally to forward events and backward events, and are termed symmetric background. However, part of the background-events were of the type $b \to \mu c(\to \mu X)$ and a fraction of these were observed to be asymmetrically distributed in θ_l. Overall, $\sim 75\% \pm 20\%$ of the background was classified as symmetric events and $\sim 25\% \pm 13\%$ was classified as asymmetric. These numbers, see table 1, were used as the basis for the analysis presented in this section. Symmetric background will not bias the FBA zero-point determination though, without correction, it will reduce the amplitude of the measured FBA distribution. Symmetric background is studied in Section 3.2. Asymmetric background, which has not been corrected for, will give rise to a bias on the zero-point determination. This potentially more significant effect is discussed

in Section 3.3.

Table 1: Background event types used as input for the FBA analysis.

Background type	Number of events/2fb^{-1}
Symmettic	827 ± 205
Asymmettric (forward)	215 ± 95
Asymmetric (backward)	70 ± 46

As the remaining number of simulated background events after selection cuts was low it was not possible to accurately evaluate the dimuon mass squared distribution of the forward events and backward events. Instead, three different distributions are used in this analysis to evaluate the effect on the FBA results. Figure 8 shows the three distributions used in the analysis. The general form of the distributions used were:

1. Signal like: a distribution of background events in $\mathrm{M}^2_{\mu^+\mu^-}$ similar to the distribution of the signal events.
2. Peak: a distribution with most background events concentrated in the $\mathrm{M}^2_{\mu^+\mu^-}$ region close to the zero point of the FBA. In the unbinned analysis, events that are far away from the zero point will have little effect on the zero point estimation, so this distribution may be expected to have a larger effect than the signal-like distribution.
3. Flat: a homogeneous distribution with background events populating the $\mathrm{M}^2_{\mu^+\mu^-}$ distribution equally.

3.1 Background Subtraction

The background was taken into account in the evaluation of the FBA distribution through the following expression:

$$FBA = \frac{(N_f^{total} f_f - N_f^{'bg} f_f^{'bg}) - (N_b^{total} f_b - N_b^{'bg} f_b^{'bg})}{(N_f^{total} f_f - N_f^{'bg} f_f^{'bg}) + (N_b^{total} f_b - N_b^{'bg} f_b^{'bg})}, \tag{1}$$

where $N_{f(b)}^{total}$ is the total number of forward (backward) events, this is the sum of the true number of signal (N^{signal}) and background (N^{bg}) events. The estimated number of background events (which is used to make the background correction) is indicated with a prime superscript as $N^{'bg}$. $f_{f(b)}$ is the true pdf as a function of the dimuon invariant mass squared evaluated using signal and background events for forward (backward) events. The corresponding term for the background with the prime superscript $f_{f(b)}^{'bg}$ is the estimated background pdf for the forward (backward) events used in the background correction.

Using the expression for f given in [1], each of the terms between brackets in expression 1 can be written in the form:

$$N_{f(b)}^{total} f_{f(b)} - N_{f(b)}^{'bg} f_{f(b)}^{'bg} = \frac{1}{h} \sum_{i=1}^{N_{f(b)}^{total}} K\left(\frac{{M_{f(b)}}^2_{\mu^+\mu^-}{}^i - {M_{f(b)}}^2_{\mu^+\mu^-}}{h}\right) - N_{f(b)}^{'bg} f_{f(b)}^{'bg}, \tag{2}$$

where i is the event index for summation over the data sample, $M^2_{\mu^+\mu^-}$ is the dimuon invariant mass squared of the event i, K is the Gaussian kernel function, and h is the smoothness parameter (see [1]).

[3] Similar results were also obtained previously in [6], and more recently in [7].

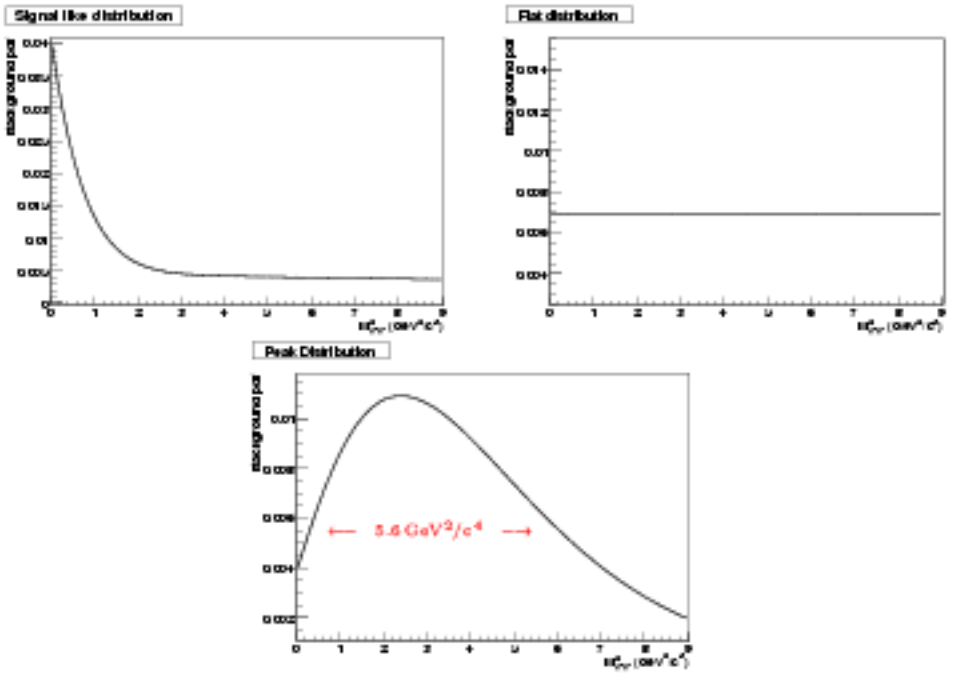

Figure 8: Background $M^2_{\mu^+\mu^-}$ distributions. Three different $M^2_{\mu^+\mu^-}$ distributions were used to evaluate the background effects. The signal-like distribution is shown on the left-hand side of the top row and the flat distribution is shown on the right-hand side of the top row. The peak distribution is shown in the bottom row. The width of the peak distribution is also illustrated.

The first term on the right-hand side of equation 2 can be broken down as:

$$\begin{aligned}\frac{1}{h}\sum_{i=1}^{N^{total}} K\left(\frac{M^{2\,i}_{\mu^+\mu^-}-M^2_{\mu^+\mu^-}}{h}\right) &= \frac{1}{h}\sum_{i=1}^{N^{signal}} K\left(\frac{M^{2\,i}_{\mu^+\mu^-}-M^2_{\mu^+\mu^-}}{h}\right)+ \\ &\quad \frac{1}{h}\sum_{j=1}^{N^{back}} K\left(\frac{M^{2\,j}_{\mu^+\mu^-}-M^2_{\mu^+\mu^-}}{h}\right) \\ &= N^{signal} f^{signal} + N^{bg} f^{bg},\end{aligned}$$

where N^{signal} is the true number of signal events and N^{bg} the true number of background events. Hence, expression 2 becomes:

$$\begin{aligned}N^{total} f - N'^{bg} f'^{bg} &= N^{signal} f^{signal} + N^{bg} f^{bg} - N'^{bg} f'^{bg} \\ &\simeq N^{signal} f^{signal},\end{aligned} \tag{3}$$

as required. The functions $N^{bg} f^{bg}$ and $N'^{bg} f'^{bg}$ should cancel out in expression 3 because they represent the true background contribution (terms without the prime superscripts) and the estimated background (terms with the prime superscripts). In LHCb N'^{bg} and f'^{bg} will be estimated from studying events from the B meson mass side-bands. In the following, equation 1 is used to obtain the FBA in the presence of background assuming both correctly estimated and mismeasured background distributions.

3.2 Symmetric Background

The effects of symmetric background on the FBA were evaluated using 300 sets of simulated background events generated from a simple 'toy' simulation. The number of background events per set was equivalent to that expected in 2 fb^{-1}, as discussed in Section 3. These data sets were used to evaluate the average values of the FBA distribution and zero point sensitivity.

Figure 9 shows the effect of symmetric background on the FBA, with and without background subtraction performed. Three different forms of the background distribution were tested. As expected, since the background is symmetric, no bias on the FBA zero point was observed when the background was not subtracted. However, a small reduction in the FBA amplitude can be seen on Figure 9.

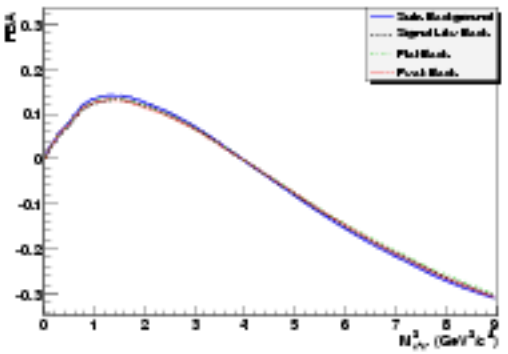

Figure 9: Effect on FBA due to symmetric background. Three different background distributions were assumed. The solid blue line corresponds to the FBA distribution with the background subtracted correctly. The dashed lines correspond to the FBA calculated for the three background distributions without background subtraction.

The sensitivity to the FBA was evaluated, having applied the background subtraction procedure. The result without background of $\sigma_{S_0} = 0.40\,\mathrm{GeV}^2/\mathrm{c}^4$ was reported in [1], this sensitivity is degraded by less than $10\,\%$ of its value in the presence of symmetric background. The sensitivity degradation obtained was $0.03\ \mathrm{GeV}^2/\mathrm{c}^4$ for all three distributions (signal-like distribution, flat background distribution, and peaked distribution).

Background Mismeasurement

The effect of mismeasuring the symmetric background was also evaluated by subtracting only a fraction of the total background. The FBA zero point value and sensitivity were calculated as a function of the fraction of background subtracted and are shown in figure 10.

As expected, no significant shift of the FBA zero point value or extra degradation of the sensitivity of the zero point measurement was observed. These results demonstrate that the FBA zero point measurement is not sensitive to the effects of symmetric background mismeasurements. This differs from the results reported from the binned method presented in [4] where the FBA zero point was shifted by $\sim 0.15\ \mathrm{GeV}^2/\mathrm{c}^4$ with a mismeasurement of 50% and its sensitivity degraded by $\sim 10\%$.

Background Increase

The bias in the FBA zero point value and the degradation of the sensitivity were also evaluated as a function of the background level. These estimates are of interest as the amount of background in the $B_d \to K^*\mu^+\mu^-$ channel could potentially be higher than that estimated with the current LHCb simulation.

Figure 11 shows the shift in the FBA zero point value and the degradation of the sensitivity as the background increases. No significant shift was observed in the FBA zero point. The degradation in sensitivity ($\sigma_{\text{Zero Point}}$) was roughly linear with $\sqrt{\text{Background(B)}/\text{Signal(S)}}$ and the slope of the curve did not depend on the background dimuon mass squared distribution.

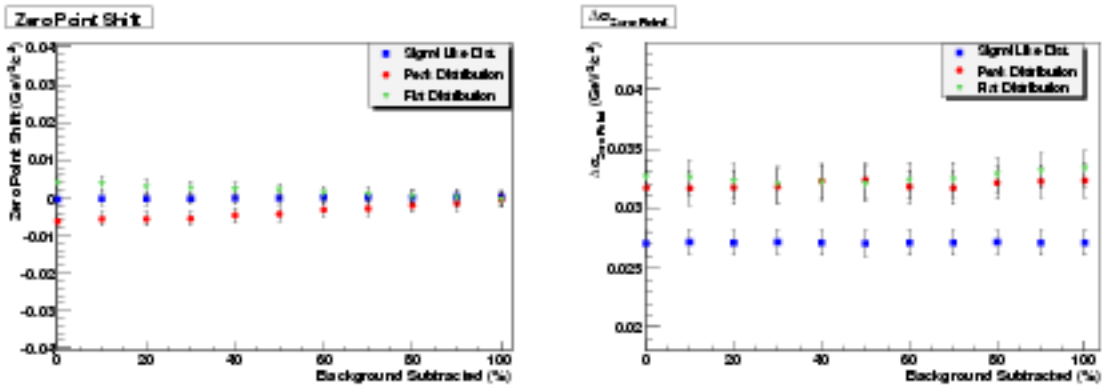

Figure 10: FBA zero point value and sensitivity as a function of the fraction of background subtracted. No significant variation in these quantities was observed.

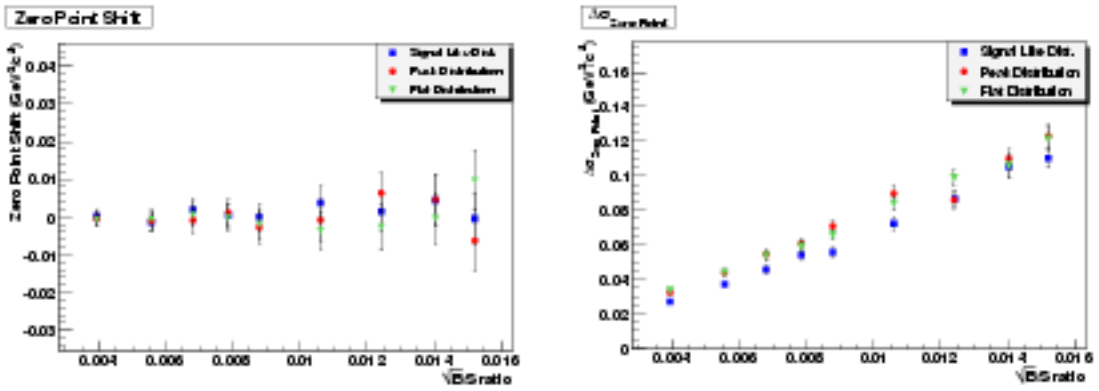

Figure 11: FBA zero point value and sensitivity as a function of the $\sqrt{B}/S$ ratio. No significant shift in the FBA zero point was observed. The degradation on the sensitivity was linear with $\sqrt{B}/S$.

3.3 Asymmetric Background

The study reported above was repeated considering the asymmetric background category. The fraction of asymmetric background obtained by a previous study in the full simulation was used (see Section 3). The FBA sensitivity was degraded by $0.01\ \mathrm{GeV}^2/\mathrm{c}^4$, $0.02\ \mathrm{GeV}^2/\mathrm{c}^4$, $0.02\ \mathrm{GeV}^2/\mathrm{c}^4$ with the signal-like, peak and flat distributions respectively. These numbers were evaluated with the correct background subtraction. Again, no significant bias in the FBA zero point was observed after background subtraction.

Although the estimated amount of asymmetric background is small when compared to the signal and to the symmetric background, the mismeasurement of this component could significantly affect the FBA. Unlike the symmetric background, the asymmetric background could potentially shift the FBA zero point. Hence, it is useful to evaluate to which precision the background has to be determined in order to avoid a significant shift of the FBA zero point.

The following procedure was implemented to evaluate the effects of the asymmetic background mismeasurement on the FBA distribution:

- The total number of asymmetric background events was not changed.
- The mismeasurement of the background level was introduced in the f^{bg} term of equation 1. This represents a mismeasurement of the background from the B_d mass side bands in the LHCb data.

- The background mismeasurement was implemented by transferring a fraction of the asymmetric background from the forward events to the backward events.

This procedure is illustrated in Figure 12. The background in the forward band and in the backward band are shown on the left-hand side of the diagram. The bars represent the value of the f distribution for a fixed dimuon mass value. The red region on the forward band shows the fraction of the background which was transferred from the forward band to the backward band to calculate the f'. The right-hand side of the diagram describes the f' distributions used with the background mismeasurement included.

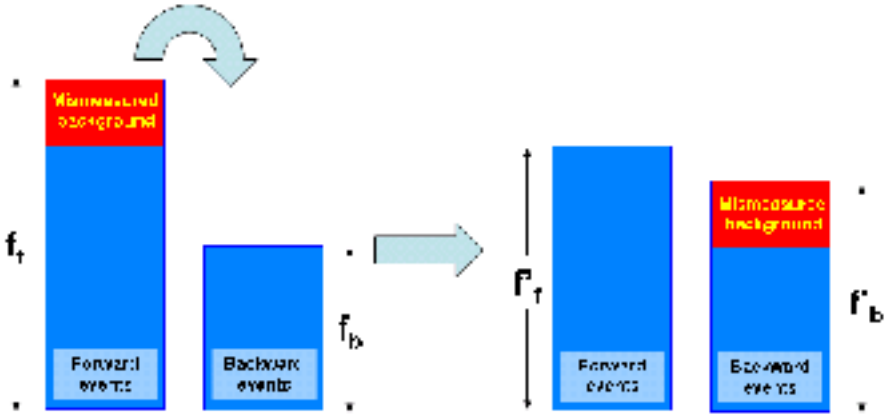

Figure 12: Diagram illustrating the asymmetric background mismeasurement algorithm. The algorithm is explained in the text.

This procedure was again performed using the three background distributions described at the start of Section 3. The same distribution was used for the forward events and backward events. Figure 13 shows the shift of the FBA zero point due to the mismeasurement of the asymmetric background component. Significant shifts can be expected, with any of the background distributions, if the mismeasurement fraction is high. With a fraction of mismeasured background of $\sim 50\%$, the shift for the peak background distribution was $\sim \sigma_{\text{ZeroPoint}} = 0.40\ \text{GeV}^2/c^4$, equivalent to the sensitivity with $2\ \text{fb}^{-1}$ data. This sets a limit on the accuracy at which the asymmetric background component must be determined.

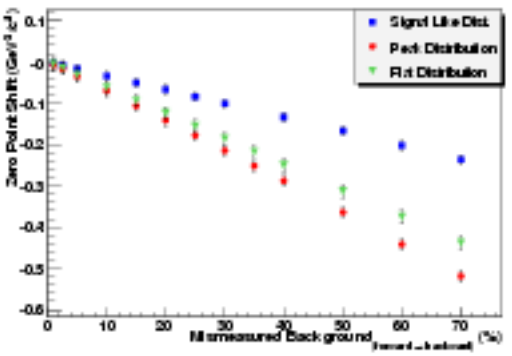

Figure 13: FBA zero point shift as a function of the fraction of asymmetric background mismeasured. The x axis represents the fraction of the asymmetric background transferred from the forward band to the backward band. The y axis is the FBA zero point shift.

Comparing the fraction of the asymmetric background with the total background level this can be converted to the minimum precision required on the total background. This minimum was calculated

as

$$\Delta_{Background} = f_{asymmetric} \times f_{mismeasured}, \quad (4)$$

where $\Delta_{Background}$ is the background uncertainty, $f_{asymmetric}$ is the fraction of the asymmetric background with respect to the total of background and $f_{mismeasured}$ is the fraction of mismeasured asymmetric background necessary to shift the zero point by about $1\sigma_{\text{Zero Point}}$ for 2fb^{-1} data. This gives $\sim \ 25\% \times 50\% = 12.5\%$. Hence, in order to avoid systematic shifts on the FBA zero point measurement dominating over the statistical error, the asymmetric background component of the $B_d \to K^*\mu^+\mu^-$ analysis should be determined with a precision better than 50%, corresponding to a precision better than 12.5% on the overall background level.

The shape of the FBA distribution is also distorted by the mismeasurement of the asymmetric background. Figure 14 shows a comparison between the FBA distribution with and without the correct background subtraction. In these distributions a 50% mismeasurement of the asymmetric background has been assumed.

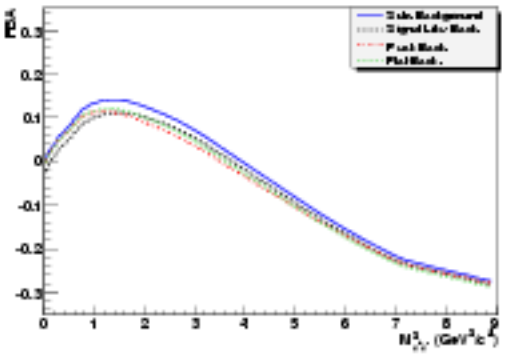

Figure 14: FBA comparison with and without asymmetric background subtraction. The solid blue line corresponds to the FBA distribution calculated subtracting the background correctly. The dashed lines correspond to the FBA calculated for the three types of background distribution with 50% mismeasurement.

4 Conclusions

A study of biases on the dimuon mass squared distribution and FBA in $B_d \to K^*\mu^+\mu^-$ was performed. Acceptance effects and background effects were considered.

The acceptance effects due to the cuts performed in the offline selection or trigger and reconstruction were evaluated. Only the cuts on the P_T of the muons were found to be significant. The muon DLL PID cut was found to be correlated with the P_T. The relative acceptance effect on the dimuon mass squared distribution was found to be significant: 15-18% at offline selection; 25-30% due to DLL and P_T cut on the muon identification; and 19-22% due to the P_T cut on L0 single muon trigger. However, as the acceptance effects were similar on both forward event and backward event distributions, the overall effect on the FBA was partially cancelled. Given the amount of simulation events available it was not possible to decide whether the FBA distribution is distorted. If there is a resulting acceptance effect on the FBA distribution it would become dominant only after $\sim 8\ \text{fb}^{-1}$ of data taking when the statistical uncertainties would become smaller than a possible bias on the FBA. A method to study the bias with high statistics in data was suggested, using muon samples from $B \to J/\psi(\mu^+\mu^-)X$ events.

The possible effects of the background on the FBA distribution were also investigated. The main effects expected on the FBA distribution were: sensitivity degradation; and distribution bias. A sensitivity degradation of only 10% for the FBA zero point is expected, given the small amount of

background which is estimated. No bias on the FBA zero point was found when the background subtraction was performed assuming the correct distributions.

The effects of background mismeasurement were also considered. For background sources that contribute equally to forward events and backward events no bias was observed and only a weak sensitivity variation. However, mismeasurement of background that contributed asymmetrically to forward events and backward events will bias the measured FBA zero point. The shape of the FBA distribution is also affected. To avoid this systematic effect dominating over the statistical error it was estimated that the asymmetric background component for the $B_d \to K^* \mu^+ \mu^-$ decay needs to be determined with a precision better than $\sim 50\%$ for 2 fb^{-1} data in LHCb.

5 Acknowledgements

We would like to thank Mitesh Patel for his suggestions and assistance with this study.

References

[1] F. Marinho et al. A non-parametric method to estimate the Forward Backward Asymmetry from the $B_d \to K^* \mu^+ \mu^-$ decay at LHCb. (CERN-LHCb-09-004).

[2] M. Patel et al. Roadmap to the measurement of the $B_d \to K^* \mu^+ \mu^-$ decay at LHCb. (CERN-LHCB-ROADMAP2-001).

[3] J. Dickens. Private communication, 2008.

[4] J. Dickens et al. Selection of the decay $B_d \to K^* \mu^+ \mu^-$ at LHCb. (CERN-LHCb-2007-038).

[5] A Algusto Alves et al. The LHCb Detector at the LHC. *JINST*, 3(S08005), 2008.

[6] J. H. Lopes. Study of the rare decay $B_d \to K^* \mu^+ \mu^-$ decay with the LHCb detector. (CERN-LHCb-2003-104).

[7] M. Patel and H. Skottowe. A cut-based selection for $B_d \to K^* \mu^+ \mu^-$. (CERN-LHCb-2009-008).